

# Poly(vinylidene fluoride-*co*-hexafluoropropene) (PVDF-HFP) membranes for ethyl acetate removal from water

Xiuzhi Tian\*, Xue Jiang

*School of Textiles & Clothing, Key Laboratory of Eco-Textiles, Ministry of Education, Jiangnan University, Wuxi 214122, China*

Received 4 March 2007; received in revised form 9 June 2007; accepted 11 August 2007

Available online 17 August 2007

## Abstract

In this study, poly(vinylidene fluoride-*co*-hexafluoropropene) (PVDF-HFP) with low crystallinity was applied as the membrane material for pervaporative separating ethyl acetate (EtAc) from its aqueous solutions. The drying conditions during membrane fabrication by means of casting the PVDF-HFP solution dominated the obtained membrane morphologies when the polar solvents such as dimethylacetamide (DMAc) and acetone were used. It was demonstrated that both the DMAc-cast and acetone-cast PVDF-HFP membranes vacuum-dried at 60 °C were dense but had different crystalline structures. Predominantly  $\alpha$  and  $\gamma$  crystalline phases were found in the acetone-cast and DMAc-cast PVDF-HFP membranes, respectively. And the different pervaporative separating performances of the two solvent-cast PVDF-HFP membranes were well explained in terms of different solution-diffusion properties which were induced from the permeants/polymer interactions on the base of the polarity differences between permeants and the two solvent-cast PVDF-HFP membranes.

© 2007 Elsevier B.V. All rights reserved.

**Keywords:** PVDF-HFP; Solvent-cast; Crystalline phase; Solution-diffusion; Pervaporative separation

## 1. Introduction

Organophilic pervaporation has a large market when it is applied into wastewater treatment or recovery of organic compounds with high value [1–3]. Membrane is the key factor dominating the separation properties of a given pervaporation process. Actually, both the choice of membrane material and the membrane preparation, which are related to the chemical and physical structures of the membrane, respectively, determine whether the aimed separation task can be accomplished by pervaporation or not. Based on the widely accepted solution-diffusion mechanism for pervaporation, hydrophobic elastomers are desirable for organophilic pervaporation considering the difference of permeating rates between the organic compounds and water [4].

Nevertheless, semi-crystalline polymer, such as poly(vinylidene fluoride) (PVDF) has been applied as the membrane material for organophilic pervaporation due to its special hydrophobicity and low surface energy [5–7]. And it is rarely studied what is the effect of crystals on the separation properties.

In this work, we adopted PVDF-HFP as the membrane material for organophilic pervaporation because it is a chemically inert fluoropolymer, has lower crystallinity compared with PVDF and good mechanical strength, can tolerate high-temperature feed solutions, and is a hydrophobic material. The aim is to obtain the correlation between the pervaporative separating properties of PVDF-HFP membrane and the existing crystals in PVDF-HFP membrane.

## 2. Experimental

### 2.1. Materials

PVDF-HFP pellets were purchased from Aldrich, USA ( $M_w=308,000$ , polydispersity index (PDI)=1.83, HFP content=5 mol%). The solvents acetone, DMAc, EtAc were reagent-grade and dried with 4 Å molecular sieve before use. Water was deionized and distilled.

### 2.2. Membrane preparation

PVDF-HFP pellets were vacuum-dried at 50 °C for 2 days and were dissolved in acetone and DMAc at 4 wt%,

\* Corresponding author.

E-mail address: [xzhtian@yahoo.com.cn](mailto:xzhtian@yahoo.com.cn) (X. Tian).

respectively. The homogeneous membranes were prepared by casting the polymer solution onto the glass plate. Two drying conditions were adopted, which were atmosphere and vacuum at 60 °C, respectively. The membrane thickness was measured using an electronic gauge in combination of the SEM photograph. Ten separate thickness measurements were taken at equal spacing around the circumference of the membrane and the average value was used.

### 2.3. Characterization of the membranes

The cross-sections of the homogeneous solvent-cast PVDF-HFP membranes were obtained by being cryogenically fractured in liquid nitrogen and then sputter coated with a 200–300 Å gold layer using a Hitachi® E120 model sputtering device. A field emission scanning electron microscope, Hitachi® S-520 was employed to view the membrane morphology.

Fourier transform infrared (FT-IR) spectroscopy of the two solvent-cast PVDF-HFP membranes were obtained by using a Bruker Vector 22 type spectrometer.

DSC tests were carried out by using of a TA® DSC Q600 analyzing system connected to a cooling system. Crystallinity ( $\chi_c$ ) of the two solvent-cast PVDF-HFP membranes could be determined by the enthalpy of fusion from DSC measurements using the calculation as

$$\chi_c (\%) = \frac{\Delta H_m}{\Delta H_m^0} \times 100 \quad (1)$$

where  $\Delta H_m$  is the fusion enthalpy of the membrane sample and  $\Delta H_m^0$  is the standard fusion enthalpy of perfectly crystalline PVDF-HFP. In this study, a value of 104.7 J/g was used for  $\Delta H_m^0$  [8].

### 2.4. Swelling measurements

The dried homogeneous PVDF-HFP membranes with known weight ( $W_{dry}$ ) were immersed in pure EtAc, thermostated in water at 25 °C for 48 h to characterize the swelling degrees. After the solution on the membrane surface was carefully removed with tissue paper, the weight of the swollen membrane ( $W_{wet}$ ) was weighed. The swelling degree (SD) of the membrane was defined by the following equation:

$$SD (\%) = \frac{W_{wet} - W_{dry}}{W_{dry}} \times 100 \quad (2)$$

where  $W_{wet}$  and  $W_{dry}$  were the weights of swollen and dry membranes, respectively.

### 2.5. Determination of diffusion coefficient

The concrete process for measuring the diffusivity at zero concentration ( $D_0$ ) was referred to Ji et al. on the assumption that the diffusion of permeating molecules in the membrane was Fickian [9].

$$\frac{d \ln (W_t - W_\infty / W_0 - W_\infty)}{dt} = \frac{\pi^2 D_0}{l^2} \quad (3)$$

where  $l$  was the membrane thickness,  $W_0$ ,  $W_t$  and  $W_\infty$  were the sample masses at time zero,  $t$  and at equilibrium, respectively.

$D_0$  could be calculated based on the desorption kinetic data analyzed for long duration with Eq. (3). In this work, the desorption kinetic data were obtained from the weight change of the solvent swollen PVDF-HFP membrane with time at 25 °C.

### 2.6. Pervaporation experiments

A traditional pervaporation apparatus was used in this study [7]. The circular flat membrane was clamped into a sealed stainless steel test cell above a porous sintered metal support with a 'o' ring arrangement forming a leak free seal, giving a pervaporation area of 28.26 cm<sup>2</sup>. The cell was filled with the feed solution and stirred at 16.66 Hz (1000 rpm) by a magnetic agitator. The cell temperature was controlled and measured with a thermocouple and electronic temperature control system, accurate to  $\pm 0.5$  °C. A vacuum pump maintained the downstream pressure at 300–400 Pa. The permeate was condensed and frozen with the cold trap, which was cooled with liquid nitrogen. The permeation rate was determined by measuring the weight of the permeate. The compositions of the feed solution and permeate were measured by gas chromatography (GC, China Chromatography 120).

Permeate flux,  $J$ , was calculated by:

$$J = \frac{Q}{At} \quad (4)$$

where  $Q$  is the total amount of the permeate passed through the membrane during an experimental time interval  $t$  at a steady state and  $A$  is the effective membrane area.

The separation factor ( $\alpha$ ) was calculated from

$$\alpha_{O/W} = \frac{Y_O/Y_W}{X_O/X_W} \quad (5)$$

where  $Y_O$ ,  $X_O$  are the weight fractions of EtAc in the permeate and feed, respectively. And  $Y_W$ ,  $X_W$  are the weight fractions of water in the permeate and feed, respectively.

Pervaporation separation index (PSI) was defined as

$$PSI = J(\alpha_{O/W} - 1) \quad (6)$$

## 3. Results and discussion

### 3.1. Choice of solvents for membrane preparation and permeants for organophilic pervaporation

It is well known that Hansen solubility parameter ( $\delta$ ) is related to the cohesive energy density generated by the van der Waal interactions. It has three components which are  $\delta_p$  due to the polar forces between molecules,  $\delta_d$  due to the molecular dispersive power, and  $\delta_h$  due to the hydrogen bonding. To characterize the solvent/polymer interaction,  $\Delta\delta_{iP}$  defined in the following equation can be used [10]:

$$\Delta\delta_{iP} = [(\delta_{pi} - \delta_{pP})^2 + (\delta_{di} - \delta_{dP})^2 + (\delta_{hi} - \delta_{hP})^2]^{1/2} \quad (7)$$

where  $i$  and  $P$  denote the solvent and polymer, respectively.

Table 1  
Solubility parameters (MPa<sup>1/2</sup>) of PVDF-HFP and solvents<sup>a</sup>

Sample	$\delta_d$	$\delta_p$	$\delta_h$	$\delta_t^b$	$\Delta\delta_{IP}$
<i>N,N</i> -Dimethylacetamide (DMAc)	16.8	11.5	10.2	22.7	2.27
Acetone	15.5	10.4	7.0	20.0	2.96
Ethyl acetate (EtAc)	15.8	5.3	7.2	18.1	7.40
Water	15.6	16.0	42.3	47.8	34.32
PVDF-HFP [11]	17.2	12.5	8.2	23.2	–

<sup>a</sup> Obtained from CRC handbook [12].

<sup>b</sup> Total solubility parameter.

Table 1 lists the solubility parameters of PVDF-HFP, water and three kinds of solvents. The  $\Delta\delta_{IP}$  values were calculated from Eq. (7) and also listed in Table 1. Based on the calculated  $\Delta\delta_{IP}$ , it is easy to estimate that acetone and DMAc can be chosen to prepare the PVDF-HFP casting solution, while EtAc can be chosen as the organic permeant for pervaporation.

### 3.2. The effect of applied conditions during membrane fabrication on the membrane morphologies

In view of the discrepancy of diffusivity between water and organic compounds through the membrane, dense or non-porous polymeric membranes are mostly used for organophilic pervaporation. In this work, the effects of applied conditions during PVDF-HFP membrane fabrication by means of solvent evaporation, such as solvent, drying condition, on the membrane morphologies were investigated. The aim was to prepare dense PVDF-HFP membrane for organophilic pervaporation successfully.

It was found that the choice of drying conditions was mostly important for obtaining the dense membranes. The morphologies of the solvent-cast PVDF-HFP membranes under two different drying conditions were presented in Figs. 1 and 2.

It can be seen from Fig. 1 that both of the cross-sections in the DMAc-cast and acetone-cast PVDF-HFP membranes dried at atmosphere are porous, while that dried at 60 °C with vacuum are dense. In consideration of the interactions between water and the casting solvents, both acetone and DMAc are polar, so they can dissolve in water. Water vapor close to the surface of the PVDF-HFP casting solution will be condensed into water with a falling of surrounding temperature due to the solvent evaporation. The condensed water will enter into the bulk of the PVDF-HFP casting solution and mixed with the solvent. Under this condition, water stayed in the bulk of the casting solution acts as a pore-former due to its weak volatility. And thus precipitation of PVDF-HFP is caused by the solvent evaporation. In this regard, the mechanism of pore formation here is different from that of solution phase inversion [13]. Moreover, the pore size bears on many factors, such as the volatility of solvent, the interaction of solvent with water, etc.

Fig. 1 shows apparently different pore sizes between the two solvent-cast PVDF-HFP membranes dried at atmosphere. The DMAc-cast PVDF-HFP membrane has larger pores than the acetone-cast one. It may be related to the lower volatility of DMAc and its stronger interaction with water.

While for membranes dried at 60 °C with vacuum, the DMAc-cast one is denser than the acetone-cast one, as seen in Fig. 2. The reason is that PVDF-HFP has higher solubil-

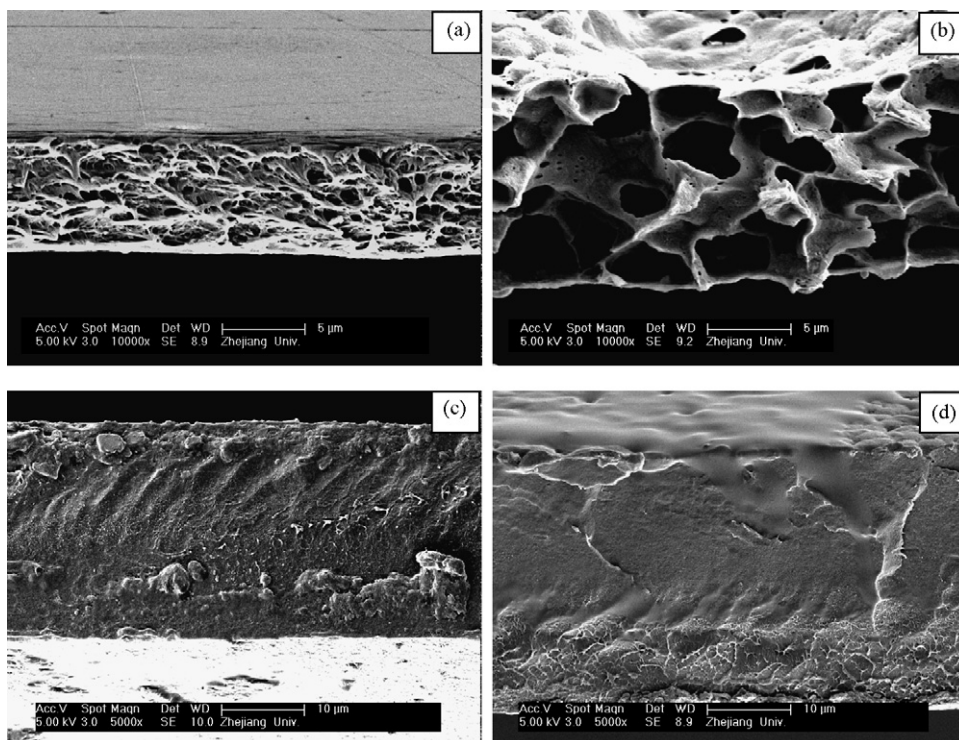


Fig. 1. SEM pictures of PVDF-HFP membranes' cross-sections prepared under different conditions. (a) acetone, atmosphere; (b) DMAc, atmosphere; (c) acetone, vacuum, 60 °C; (d) DMAc, vacuum, 60 °C.

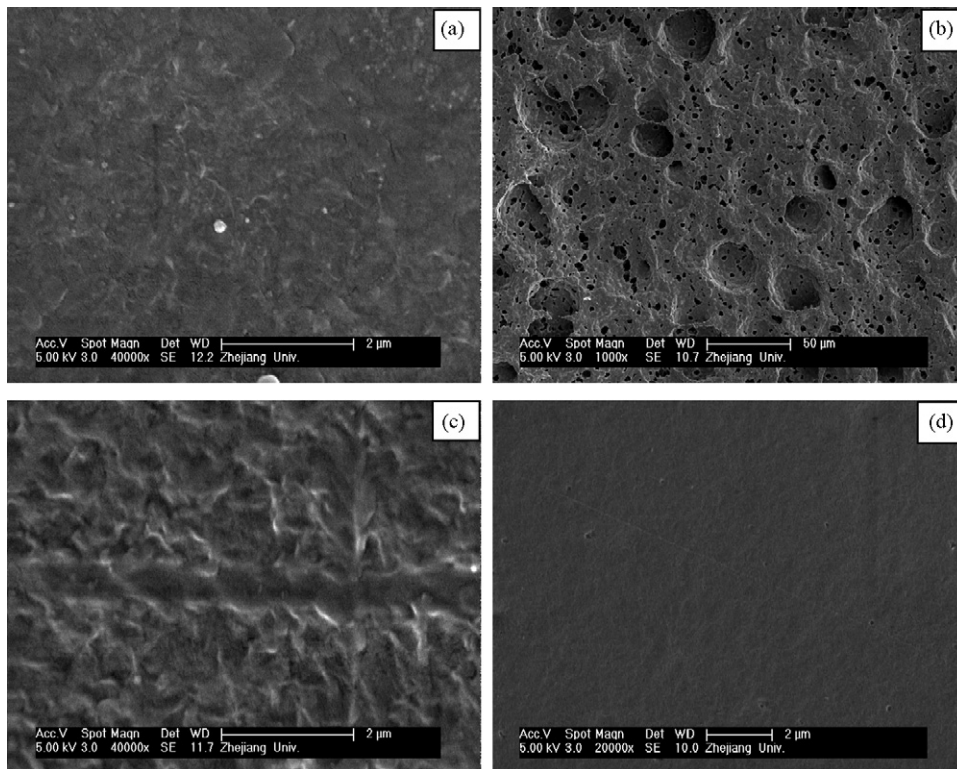


Fig. 2. SEM pictures of the solvent-cast PVDF-HFP membranes' surfaces prepared under different drying conditions. (a) acetone, atmosphere; (b) DMAc, atmosphere; (c) acetone, vacuum, 60 °C; (d) DMAc, vacuum, 60 °C.

ity in DMAc than in acetone, bringing on its more extended macromolecular chains in DMAc and closer arrangements.

Fig. 2 also presents dense surface in the acetone-cast PVDF-HFP membranes regardless of its drying condition. It may be resulted from the high volatility of acetone. In fact, even though the acetone-cast PVDF-HFP membrane dried at atmosphere seems to satisfy for organophilic pervaporation, it is too breakable to meet the intensity requirement due to the large pores existing in the bulk of this membrane.

### 3.3. The different crystalline structures of the two solvent-cast PVDF-HFP membranes

It is well known that PVDF can crystallize mainly to three structures:  $\alpha$ ,  $\beta$ , and  $\gamma$  type (or forms  $\Pi$ , I, III). These crystalline structures have been characterized extensively in the literature [14,15].

FT-IR spectrum is an important method extensively used for characterizing the different crystalline phases of homo PVDF and its copolymers, i.e. PVDF-HFP [16]. Fig. 3 shows the FT-IR spectra of the two solvent-cast PVDF-HFP membranes which were isothermally dried at 60 °C with vacuum. An almost predominance of  $\alpha$  crystalline phase is observed in the acetone-cast PVDF-HFP membrane according to the presence of absorption apices at 531, 614, 763, 796, 854, 878, and 976  $\text{cm}^{-1}$  [17,18].

Although the absorption apices of the monoclinic  $\gamma$  phase are in accordance with that of the orthorhombic  $\beta$  phase, two characteristic absorption apices at 812 and 882  $\text{cm}^{-1}$  are used as a good means for identification of  $\gamma$  phase [19,20]. Furthermore,

an absence of the characteristic absorption apices of  $\beta$  phase at 1286 or 1431  $\text{cm}^{-1}$  but an appearance of the absorption apex of the characteristic  $\gamma$  phase at 1234  $\text{cm}^{-1}$  in the FT-IR spectrum of the DMAc-cast PVDF-HFP membrane, Fig. 3, account for the apices at 510 and 839  $\text{cm}^{-1}$  being assigned to  $\gamma$  phase. In conclusion, a main presence of  $\gamma$  phase in the DMAc-cast PVDF-HFP membrane is assured due to the presence of the absorption apices at 510, 812, 839, 882 and 1234  $\text{cm}^{-1}$ .

To date, the reason about the different behavior of the two studied polymer–solvent systems mentioned above has not been

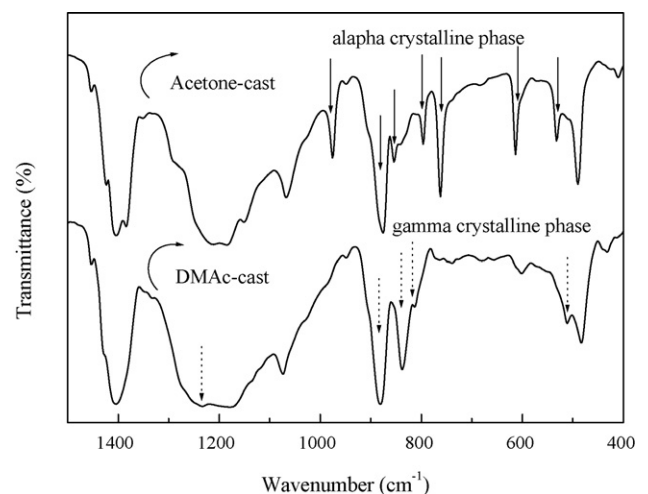


Fig. 3. FT-IR spectra of the two solvent-cast PVDF-HFP membranes dried at 60 °C with vacuum.

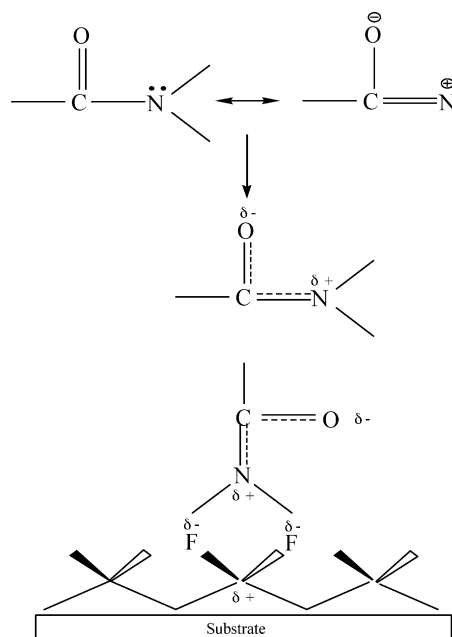


Fig. 4. Schematic view of dipolar intermolecular interactions between PVDF-HFP and DMAc.

clearly explained yet. However, a reasonable explanation is available from Salimi and Yousefi based on the polymer–solvent interactions [21]. Fig. 4 illustrates a schematic representation of the dipolar intermolecular interactions between PVDF-HFP and DMAc.

The extreme electronegativity of fluorine atom (4) compared with that of carbon atom (2.5) ensures a strong polarized interatomic C–F bond so that the bond carries a permanent strong electric moment. And a strong electron resonance between nitrogen and the neighboring carbonyl group exists in DMAc. Therefore, polar moieties of DMAc tend to rotate the strong dipoles of C–F bonds around C–C bonds of chain backbone so that more expanded chain coil and intermediately trans-conformation (*TTTGTTG*) is induced during polymer crystallization. Polar moieties of DMAc negative charged will be attracted by the positive charged surface of PVDF-HFP unit, which can reduce the energy required to form the polar crystal ( $\gamma$  phase) but there is no effect on a non-polar crystal ( $\alpha$  phase). Nevertheless, electron resonance in acetone is difficult to occur, resulting in almost no dipolar intermolecular interactions in the PVDF-HFP–acetone system, and thus trans-conformation is impossible to form.

#### 3.4. The swelling and diffusive properties of the two solvent-cast PVDF-HFP membranes

The dependence of diffusivity ( $D$ ) on the concentration and temperature can be expressed with the following equations [22]:

$$D = D_0 \exp(\gamma C) \quad (8)$$

$$D = D_0 \exp \left[ -\frac{E_D}{RT} \right] \quad (9)$$

where  $D_0$  is the diffusivity at zero concentration,  $\gamma$  the plasticizing coefficient,  $C$  the concentration of the permeating molecules in the membrane,  $E_D$  the activation energy of diffusion,  $R$  the universal gas constant, and  $T$  is the temperature.

Eqs. (8) and (9) imply that  $D_0$  is independent of the concentration ( $C$ ) and temperature ( $T$ ), so it is a good parameter to characterize the diffusivity for the investigated permeant/polymer system.

The experimental results from  $D_0$  tests were listed in Table 2. Otherwise, that from the swelling and DSC measurements were also listed in Table 2.

It can be seen that each of water and EtAc has evidently different solubility in the two solvent-cast PVDF-HFP membranes. It cannot be only explained from the viewpoint of the different contents of the amorphous region in the two solvent-cast PVDF-HFP membranes shown in Table 2 are approximate. Nevertheless, it can be perfectly explained from the interaction point of view based on the polarity difference between the permeants and solvent-cast PVDF-HFP membranes.

The  $\alpha$  crystalline phase in the acetone-cast PVDF-HFP membrane is nonpolar, while the  $\gamma$  crystalline phase in the DMAc-cast one is polar [14]. As a result, as far as the polarity difference between the permeant and the polymeric membrane is concerned, EtAc as the organic permeant in pervaporation has various affinities for the two solvent-cast PVDF-HFP membranes. The smaller polarity difference between EtAc and the acetone-cast PVDF-HFP membrane makes for stronger interaction between them, and thus an obviously higher EtAc solubility but a smaller diffusion coefficient of EtAc in this membrane appear, as seen in Table 2.

As the other permeant in pervaporation, water also has different solubilities in the two solvent-cast PVDF-HFP membranes. The reason bears on both the different contents of the amorphous region and the different crystalline phases in these membranes. That is, the stronger interaction between polar water and the DMAc-cast PVDF-HFP membrane containing polar  $\gamma$  crystalline phase, adding on somewhat higher content of amorphous region in the DMAc-cast PVDF-HFP membrane contributes to the higher water sorption in this membrane, presented in Table 2.

#### 3.5. The different pervaporation performances of the two solvent-cast PVDF-HFP membranes

According to the commonly accepted solution-diffusion mechanism for organophilic pervaporation, the separation prop-

Table 2

The crystalline, swelling and diffusive properties of the two solvent-cast PVDF-HFP membranes dried at 60 °C with vacuum

Membrane sample	$\chi_c^a$ (%)	SD in pure water (%)	SD in pure EtAc (%)	$D_0$ ( $\times 10^{11}$ m <sup>2</sup> /s)
Acetone-cast	23.6	6.4	133	2.13
DMAc-cast	21.5	10.7	22	2.99

<sup>a</sup> Crystallinity estimated from DSC measurement (%).

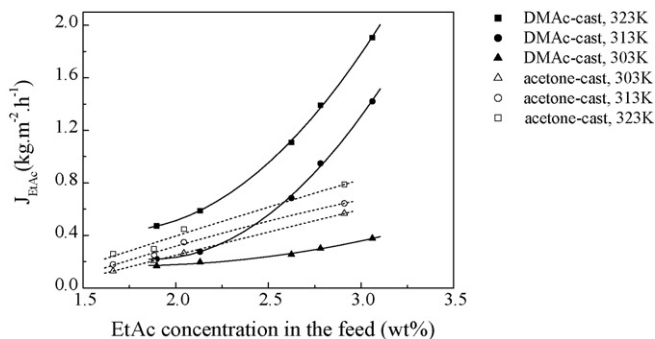


Fig. 5. Effect of the feed concentration and temperature on the EtAc permeate flux in pervaporation of the EtAc/water mixtures. The membrane was dried at 60 °C with vacuum and 10  $\mu\text{m}$  thick.

erties of an organophilic pervaporation process are determined by the different permeabilities of the permeating components through the membrane which combine the influence of sorption and diffusion steps [23].

As is well known that an organophilic pervaporation process is influenced by the operational variables such as the feed temperature, feed concentration, permeate pressure, feed flow dynamics, module geometry, and so on. The evaluation and understanding of these variables are always important for achieving the effective separation. Generally, the effect of the operational variables has been reported in terms of the permeate flux and separation factor.

In this study, the effects of two operational variables, which are the feed temperature and feed concentration, on the pervaporative separation performances (EtAc permeate flux, water permeate flux and separation factor) of the two solvent-cast PVDF-HFP membranes at a fixed permeate pressure were illustrated in Figs. 5–7. It is obvious that their pervaporative behaviors when in contact with the EtAc/water mixtures are basically different. An infrequent phenomena can be interestingly found that the separation factor of the DMAC-cast PVDF-HFP membrane increases with the feed concentration.

It can be seen from Figs. 5–7 that both of the EtAc and water permeate fluxes increase with an increase in either feed temperature or feed concentration, and the separation factor decreases

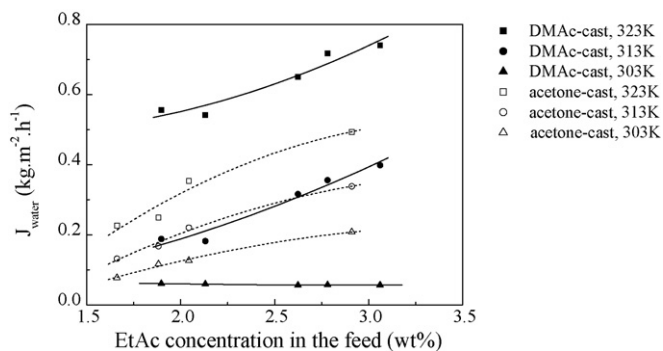


Fig. 6. Effect of the feed concentration and temperature on the water permeate flux in pervaporation of the EtAc/water mixtures. The membrane was dried at 60 °C with vacuum and 10  $\mu\text{m}$  thick.

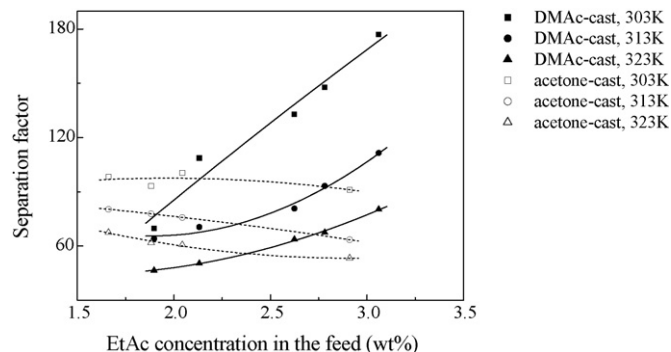


Fig. 7. Effect of the feed concentration and temperature on the separation factor in pervaporation of the EtAc/water mixtures. The membrane was dried at 60 °C with vacuum and 10  $\mu\text{m}$  thick.

with an increase of the feed temperature. However, the changed extents of the permeate fluxes between water and EtAc, as well as that of separation factor varied. This relies on the permeants' properties and their interactions with the membrane, reflected as the different sorption and diffusion properties.

The relations of the solubility and diffusivity with the temperature can be exhibited according to Arrhenius Eqs. (9) and (10) [2,24]:

$$S = S_0 \exp \left[ \frac{\Delta H_S}{RT} \right] \quad (10)$$

In Eq. (10)  $S_0$  represents the solubility at a reference state;  $\Delta H_S$  is the enthalpy of dissolution of the permeant in the membrane. On the one hand, the sorption process is generally exothermic, so that  $\Delta H_S$  is negative and, accordingly, the sorption coefficients usually decrease with the temperature [25]. Diffusion, on the other hand, is favored upon a temperature increase because of the greater kinetic energy of the permeant and the larger available free volume in the polymeric matrix [26–28]. All the above-mentioned analyses illuminate that an increase of both the water and EtAc permeate fluxes with the temperature are essentially ascribed to an improvement of the diffusivity. Moreover, the driving force for pervaporation itself is temperature dependent, since both the vapor pressure and the activity coefficient of the permeating species, and hence their chemical potentials, increase as the temperature grows.

As is discussed, EtAc has weaker interaction with the DMAC-cast PVDF-HFP membrane, resulting in its higher diffusivity coefficient ( $D_0$ ) through and smaller sorption in this membrane than in the acetone-cast one. Accordingly, based on Eqs. (8) and (9), the diffusivity ( $D$ ) for the EtAc/DMAC-cast PVDF-HFP membrane system has higher relativity with the feed temperature and concentration.

At 30 °C feed temperature and in the investigated range of feed concentration, an obviously smaller sorption of EtAc in the DMAC-cast PVDF-HFP membrane and the constantly low temperature confine the exertion of the potentially better diffusivity ( $D$ ) of EtAc through the DMAC-cast PVDF-HFP membrane in spite of the higher  $D_0$  for this permeant/polymeric membrane system. Hence, the EtAc permeate flux for the DMAC-cast PVDF-HFP membrane shows a smaller increasing trend with the

feed concentration in comparison with that for the acetone-cast one, as seen in Fig. 5.

However, at the constantly higher feed temperature (40, 50 °C), the DMAc-cast PVDF-HFP membrane shows a more apparent increasing trend of EtAc permeate flux with the feed concentration than the acetone-cast one, presented in Fig. 5. It implies that an improvement of the diffusivity ( $D$ ) of EtAc through the DMAc-cast PVDF-HFP membrane spurs an increase of sorption rate of EtAc in this membrane. This is just the reason accounting for an increase of separation factor with the feed concentration when the DMAc-cast PVDF-HFP membrane is in pervaporation of the EtAc/water mixtures at relatively higher temperatures (40, 50 °C), as indicated in Fig. 7.

Fig. 5 also shows that compared with the EtAc permeate flux for the acetone-cast PVDF-HFP membrane, that for the DMAc-cast one increases to a larger extent with the feed temperature. This is just rooted in an evident improvement of the diffusivity ( $D$ ) with the feed temperature.

It is well known that water can diffuse through the membrane more easily than EtAc due to its smaller molecular volume. Nevertheless, the permeate flux of water is much lower than that of EtAc because water has a much lower solubility in the membrane and thus the preferential permeation of EtAc comes true. When the membrane contacts the EtAc/water mixtures, the hydrophobicity of the membrane surface is reduced due to EtAc's sorption, so water sorption is possible. Moreover, with an increase of the feed concentration, water sorption increases, resulting in an increase of the water permeate flux, as presented in Fig. 6. Certainly, when the feed temperature is enhanced, the water permeate flux appears an obvious increase due to the improved diffusivity of water, and even its increased extent is higher than the EtAc permeate flux, inducing a decrease of the separation factor, as seen in Fig. 7.

Fig. 6 also shows a varied trend of the water permeate flux between the two solvent-cast PVDF-HFP membranes with the feed concentration and temperature. As mentioned before,  $\gamma$  crystalline phase in the DMAc-cast PVDF-HFP membrane potentially helps to the water sorption due to the stronger interaction between them. Nevertheless, at a constantly low temperature (30 °C), the mobility of water molecules is restrained instead by their affinity for this membrane, so the water permeate flux for the DMAc-cast PVDF-HFP membrane presents a lower value in comparison with that for the acetone-cast one, and even exhibits a decreasing trend with the feed concentration. Under this condition, the separation factor increases with the feed concentration, as seen in Fig. 7. With the feed temperature increasing, the mobility of the water molecules is accelerated, a more evident increase of the permeate water flux for the DMAc-cast PVDF-HFP membrane is resulted, as shown in Fig. 6.

Fig. 8 presents the PSI values of the two solvent-cast PVDF-HFP membranes. In general, the PSI value of the DMAc-cast PVDF-HFP membrane is higher than that of the acetone-cast one, which suggests that to obtain higher separation performance of a given polymeric membrane material, PVDF-HFP, it is important for us to control the preparation conditions, especially the casting solvent.

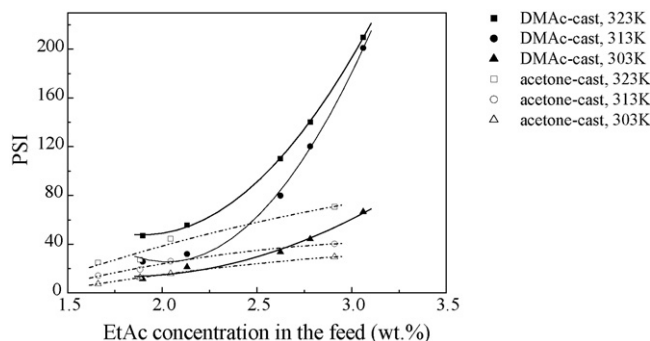


Fig. 8. Comparison of PSI value between the two solvent-cast PVDF-HFP membranes in pervaporation of EtAc/water mixtures. The membrane was dried at 60 °C with vacuum and 10  $\mu$ m thick.

#### 4. Conclusion

The drying conditions during the fabrication of PVDF-HFP membranes by means of solvent evaporation dominated the obtained membrane morphologies when the polar solvents such as DMAc and acetone were adopted for preparing the casting solutions. The PVDF-HFP membranes dried at atmosphere were porous while that dried at 60 °C with vacuum were dense.

An almost predominance of  $\alpha$  crystalline phase was observed in the acetone-cast PVDF-HFP membranes and a main presence of  $\gamma$  crystalline phase was found in the DMAc-cast PVDF-HFP membranes. The larger polarity difference between EtAc and the DMAc-cast PVDF-HFP membrane made for weaker interaction between them, resulting in an obviously smaller solubility of EtAc in this membrane and a higher diffusion coefficient at zero concentration for this permeant/polymeric membrane system.

Obviously different performances appeared between the two solvent-cast PVDF-HFP membranes when in pervaporation of the EtAc/water mixtures. It was interesting to find for the DMAc-cast PVDF-HFP membrane, its separation factor increased with the feed concentration. At the constantly low temperature (30 °C), it was mainly attributed to the confined water permeate fluxes, while at the relatively higher temperature (40, 50 °C), it could be explained from an increase of the sorption rate resulting from an increase of the diffusivity.

Higher PSI value of the DMAc-cast PVDF-HFP membrane than that of the acetone-cast one indicates that DMAc is more suitable for preparing the PVDF-HFP casting solution.

#### Acknowledgement

This work was supported by the Open Project Program of Key Laboratory of Eco-Textiles, Ministry of Education, China (No. KLET0612).

#### References

- [1] F. Lipnizki, S. Hausmanns, P.-K. Ten, R.W. Field, G. Laufenberg, Organophilic pervaporation: prospects and performance, *Chem. Eng. Sci.* 73 (2) (1999) 113–129.
- [2] X.S. Feng, R.Y.M. Huang, Liquid separation by membrane pervaporation: a review, *Ind. Eng. Chem. Res.* 36 (4) (1997) 1048–1066.

- [3] M. Peng, L.M. Vane, S.X. Liu, Recent advances in VOCs removal from water by pervaporation, *J. Hazard. Mater.* 98 (1–3) (2003) 69–90.
- [4] K. Jian, P.N. Pintauro, Asymmetric PVDF hollow-fiber membranes for organic/water pervaporation separations, *J. Membr. Sci.* 135 (1) (1997) 41–53.
- [5] K. Jian, P.N. Pintauro, R. Ponangi, Separation of dilute organic/water mixtures with asymmetric poly(vinylidene fluoride) membranes, *J. Membr. Sci.* 117 (1–2) (1996) 117–133.
- [6] K. Jian, P.N. Pintauro, Integral asymmetric poly(vinylidene fluoride) (PVDF) pervaporation membranes, *J. Membr. Sci.* 85 (3) (1993) 301–309.
- [7] M. Khayet, G. Chowdhury, T. Matsuura, Surface modification of poly(vinylidene fluoride) pervaporation membranes, *AIChE J.* 48 (12) (2002) 2833–2843.
- [8] M. Tazaki, R. Wada, M. Okabe, T. Homma, Crystallization and gelation of poly(vinylidene fluoride) in organic solvents, *J. Appl. Polym. Sci.* 65 (8) (1997) 1517–1524.
- [9] W. Ji, S.K. Sikdar, S.T. Hwang, Sorption, diffusion and permeation of 1,1,1-trichloroethane through adsorbent-filled polymeric membranes, *J. Membr. Sci.* 103 (3) (1995) 243–255.
- [10] D.R. Lloyd, T.B. Meluch, *Materials Science of Synthetic Membranes*, American Chemical Society, 1985.
- [11] A. Bottino, G. Capannelli, S. Munari, A. Turturro, Solubility parameters of poly(vinylidene fluoride), *J. Polym. Sci. Pol. Phys.* 26 (1988) 785–794.
- [12] A.F.M. Barton, *CRC Handbook of Solubility Parameters and Other Cohesion Parameters, Practical Liquid Solubility Scales*, CRC, Boca Raton, FL, 1983, pp. 139–200 (Chapter 8).
- [13] M.H.V. Mulder, *Basic Principle of Membrane Technology*, Kluwer Academic, Dordrecht, 1992.
- [14] R. Hasegawa, Y. Takahashi, Y. Chatani, H. Tadokoro, Crystal structures of three crystalline forms of poly(vinylidene fluoride), *Polym. J.* 3 (5) (1972) 600–610.
- [15] M. Kobayashi, K. Tashiro, H. Tadokoro, Molecular vibrations of three crystal forms of poly(vinylidene fluoride), *Macromolecules* 8 (2) (1975) 158–171.
- [16] A. Dikshit, A.K. Nandi, Thermoreversible gelation of poly(vinylidene fluoride) in diesters: influence of intermittent length of morphology and thermodynamics of gelation, *Macromolecules* 33 (35) (2000) 2616–2625.
- [17] M. Benz, W.B. Euler, O.J. Gregory, The role of solution phase water on the deposition of thin films of poly(vinylidene fluoride), *Macromolecules* 35 (7) (2002) 2682–2688.
- [18] R. Gregorio, J.M. Cestari, Effect of crystallization temperature on the crystalline phase content and morphology of poly(vinylidene fluoride), *J. Polym. Sci. Pol. Phys.* 32 (5) (1994) 859–870.
- [19] K. Matsushige, K. Nagata, S. Imada, T. Takemura, The II–I crystal transformation of poly(vinylidene fluoride) under tensile and compressional stresses, *Polymer* 21 (12) (1980) 1391–1397.
- [20] D.T. Grubb, K.W. Choi, The annealing of solution grown crystals of alpha and gamma poly (vinylidene fluoride), *J. Appl. Phys.* 52 (10) (1981) 5908–5915.
- [21] A. Salimi, A.A. Yousefi, Conformational changes and phase transformation mechanisms in PVDF solution-cast films, *J. Polym. Sci. Pol. Phys.* 42 (2004) 3487–3495.
- [22] C.K. Yeom, H.K. Kim, J.W. Rhim, Removal of trace VOCs from water through PDMS membranes and analysis of their permeation behaviors, *J. Appl. Polym. Sci.* 73 (4) (1999) 601–611.
- [23] J.G. Wijmans, R.W. Baker, The solution-diffusion model: a review, *J. Membr. Sci.* 107 (1–2) (1995) 1–21.
- [24] J. Néel, Pervaporation, in: R.D. Noble, S.A. Stern (Eds.), *Membrane Separation Technology—Principles and Applications*, Elsevier Inc., Amsterdam, 1995, pp. 143–211.
- [25] C. Dotremont, B. Brabants, K. Geeroms, J. Mewis, C. Vandecasteele, Sorption and diffusion of chlorinated hydrocarbons in silicalite-filled PDMS membranes, *J. Membr. Sci.* 104 (1–2) (1995) 109–117.
- [26] S.B. Kulkarni, M.Y. Kariduraganavar, T.M. Aminabhavi, Sorption, diffusion, and permeation of esters, aldehydes, ketones and aromatic liquids into tetrafluoroethylene/propylene at 30, 40, and 50°C, *J. Appl. Polym. Sci.* 89 (12) (2003) 3201–3209.
- [27] N. Vahdat, Estimation of diffusion coefficient for solute–polymer systems, *J. Appl. Polym. Sci.* 42 (12) (1991) 3165–3171.
- [28] S.V. Satyanarayana, A. Sharma, P.K. Bhattacharya, Composite membranes for hydrophobic pervaporation: study with the toluene–water system, *Chem. Eng. J.* 102 (2) (2004) 171–184.